Separation Science and Technology
Publication details, including instructions for authors and subscription information:
http://www.informaworld.com/smpp/title~content=t713708471

A Pseudophase-Change Solution-Diffusion Model for Pervaporation. II. Binary Mixture Permeation

Jyh-Jeng Shieh; Robert Y. M. Huang

To cite this Article Shieh, Jyh-Jeng and Huang, Robert Y. M.(1998) 'A Pseudophase-Change Solution-Diffusion Model for Pervaporation. II. Binary Mixture Permeation', Separation Science and Technology, 33: 7, 933 — 957

To link to this Article: DOI: 10.1080/01496399808545000

URL: http://dx.doi.org/10.1080/01496399808545000

SEPARATION SCIENCE AND TECHNOLOGY, 33(7), pp. 933–957, 1998

A Pseudophase-Change Solution-Diffusion Model for Pervaporation. II. Binary Mixture Permeation

---

JYH-JENG SHIEH and ROBERT Y. M. HUANG*
DEPARTMENT OF CHEMICAL ENGINEERING
UNIVERSITY OF WATERLOO
WATERLOO, ONTARIO N2L 3G1, CANADA

ABSTRACT

On the basis of solution-diffusion mechanism and incorporation of a pseudophase-change phenomenon, the pseudophase-change solution-diffusion (PPCSD) model is developed for pervaporation of a binary mixture through a membrane system. Flux equations of individual components thus derived clearly describe the role of coupling flux in pervaporation and show that it depends mainly on the solubility and mobility of the other component in the membrane. Good agreement is found between the theoretical and experimental results (from literature values for the hexane–heptane–polyethylene system). In addition to the solubility and mobility of individual component, the pervaporation performance of a membrane is influenced by the effect of plasticization and coupling flux, especially when strong interaction, occur between the permeants and the membrane. A parameter study indicates that both plasticizing and coupling effects enhance the permeation rate and usually lead to a decrease in membrane permselectivity.

Key Words. Pervaporation; Pseudophase-change solution-diffusion model; Binary mixture permeation; Plasticizing effect; Coupling flux

INTRODUCTION

Pervaporation is a membrane process used to separate liquid mixtures by applying vacuum at one side of membrane as the driving force. The transport

---

* To whom correspondence should be addressed.

of mixtures through a polymeric membrane is generally much more complex because the systems are often highly interactive. Therefore, two phenomena have to be distinguished in multicomponent permeation in pervaporation; flow coupling and thermodynamic interaction leading to preferential sorption and diffusion. Much effort has been devoted to the development of a satisfactory mass transport model for pervaporation. Three approaches to describe the permeation process of pervaporation can be found in the literature: the solution-diffusion model, the pore flow model, and irreversible thermodynamics.

The separation and permeation of components, as described in the solution-diffusion model, is governed by thermodynamically based sorption and kinetically based diffusion. Formulating from a fundamental mass transport equation, namely Fick's law, much attention has been given to find an adequate expression for solubility and diffusivity in the membrane. In solubility modeling, an empirical equation of activity-dependent solubility (1–4) as well as a molecular theory such as Flory–Huggins thermodynamics (6–11), UNIQUAC model (12, 13), and penetrant solubility model (14) have been utilized. In another approach, empirical expressions of linear (1, 2, 4, 5) or exponential (10, 15–18) concentration-dependent diffusivity, Fujita's free volume theory (6–9), and a hybrid diffusivity model (14) were applied to the diffusion process. The successful interpretation of mutual interaction between permeants and the membrane makes the solution-diffusion model the most accepted mass transport mechanism for pervaporation.

However, various other transport mechanisms have been proposed as an alternative to the solution-diffusion model to illustrate some important features of pervaporation. The pore flow model (19–22), which describes pervaporation as liquid permeation followed by vapor permeation through tiny pores due to the pressure difference between the two ends of a pore, has been used to investigate several mixture/membrane systems. Although the definition of pore may raise some controversy, the pore flow model attempts to explain the phenomenon of phase change of permeating species. Tyagi and Matsuura et al. (23–25) provided another approach to describe the phase change of permeant in a membrane by using a chemical potential gradient as the driving force, and they predicted a possibility of concentration polarization inside the membrane during steady-state pervaporation. On the other hand, a theoretical pervaporation model based on irreversible thermodynamics (26, 27) manifestly reveals that the coupling flux of binary mixtures in pervaporation results from the driving force of the other component. All the above-mentioned pervaporation models attempt to interpret some aspects of the pervaporation process.

In our prior paper (28) the fundamental framework of the pseudophase-change solution-diffusion (PPCSD) model for pure component pervaporation was developed. Extension of the PPCSD model to binary mixture pervaporation is demonstrated in this paper. The validity of this model for binary mixture permeation is tested using experimental data of the hexane–heptane–polyethylene system from the literature (2), and a parameter analysis of the effect of membrane plasticization and coupling flux on the membrane is also presented.

THEORY

Mass Transport through the Membrane System

Binary mixture permeation through a membrane system can be considered to be a ternary membrane system consisting of components i, j, and the polymer itself. The mass balance for this system can be given as (29) follows. For Component i:

$$n_i = \omega_i(n_i + n_j + n_p) + n_{iD} \tag{1}$$

For Component j:

$$n_j = \omega_j(n_i + n_j + n_p) + n_{jD} \tag{2}$$

For the polymer:

$$n_p = 0 \text{ (stationary)} \tag{3}$$

where n_i, n_j, and n_p are the mass flux of Components i, j, and polymer through the membrane system, respectively. ω_i and ω_j are the mass fractions of Components i and j in the membrane system, respectively. n_{iD} and n_{jD} are the mass fluxes of Components i and j through the membrane system due to diffusion. To solve n_i and n_j in terms of n_{iD} and n_{jD}, we obtain

$$n_i = \frac{1 - \omega_j}{1 - \omega_i - \omega_j} n_{iD} + \frac{\omega_i}{1 - \omega_i - \omega_j} n_{jD} \tag{4}$$

$$n_j = \frac{\omega_j}{1 - \omega_i - \omega_j} n_{jD} + \frac{1 - \omega_i}{1 - \omega_i - \omega_j} n_{jD} \tag{5}$$

The diffusion fluxes of Components i and j are, respectively,

$$n_{iD} = -\rho_i m_i \frac{d\mu_i}{dx} \tag{6}$$

$$n_{jD} = -\rho_j m_j \frac{d\mu_j}{dx} \tag{7}$$

where ρ_i and ρ_j are the concentrations, m_i and m_j are the mobilities, and μ_i and μ_j are the chemical potentials of Components i and j in the membrane system, respectively.

By substituting Eqs. (6) and (7) into Eqs. (4) and (5), respectively, we obtain

$$n_i = -\frac{1 - \omega_j}{1 - \omega_i - \omega_j} \rho_i m_i \left(\frac{d\mu_i}{dx}\right) - \frac{\omega_i}{1 - \omega_i - \omega_j} \rho_j m_j \left(\frac{d\mu_j}{dx}\right) \tag{8}$$

$$n_j = -\frac{1 - \omega_i}{1 - \omega_i - \omega_j} \rho_j m_j \left(\frac{d\mu_j}{dx}\right) - \frac{\omega_j}{1 - \omega_i - \omega_j} \rho_i m_i \left(\frac{d\mu_i}{dx}\right) \tag{9}$$

where

$$\omega_i = \frac{c_i}{1 + c_i + c_j} \tag{10}$$

$$\omega_j = \frac{c_i}{1 + c_i + c_j} \tag{11}$$

$$\rho_i = \frac{c_i d_m}{1 + c_i + c_j} \tag{12}$$

$$\rho_j = \frac{c_j d_m}{1 + c_i + c_j} \tag{13}$$

where d_m is the density of the membrane system and assumes a constant value (28); c_i and c_j are the solubility of components i and j in the membrane, respectively.

The flux equations, Eqs. (8) and (9), clearly describe the role of the coupling flux in pervaporation. The first term of the two equations on the right-hand side describes the mass flux of permeants due to their own chemical potential gradient. The second term of both equations on the right-hand side represents the coupling flow resulting from the other chemical potential gradient.

Pervaporation Flux of Individual Component through the Membrane System

The Pseudophase-change solution-diffusion model (28) assumes that the permeation mechanism through the membrane system is composed of liquid permeation and vapor permeation mechanisms in series as described in Fig. 1. The following assumptions are also made:

1. The permeation of components through the membrane system follows the solution-diffusion mechanism in both the liquid permeation process and the vapor permeation process.
2. Thermodynamic equilibrium exists at both interfaces of the membrane system.

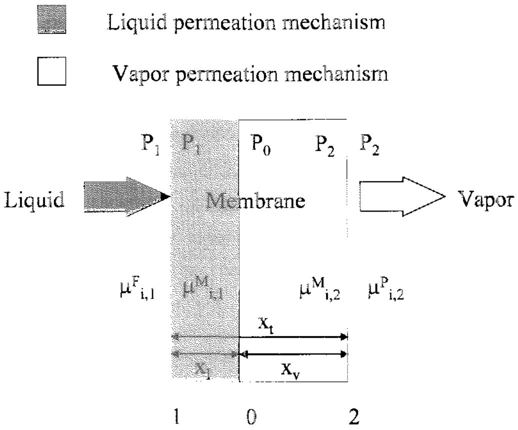

FIG. 1 Schematic description of the Pseudophase-change solution-diffusion (PPCSD) model.

3. The components undergo a pseudophase change, from liquid permeation mechanism to vapor permeation mechanism, within the membrane system during pervaporation operation.
4. The pressure at the interface of the membrane system is equal to the adjacent applied pressure.
5. It is assumed that the pervaporation process is isothermal.

In the zone that behaves as a liquid permeation process, the chemical potential of Component i in an isothermal membrane system can be written as

$$\mu_i = \mu_{i0} + RT \ln a_i + \int_{P_0}^{P} V_i dP \tag{14}$$

where μ_{i0} is the chemical potential of Component i in the membrane system at reference state, a_i is the activity of Component i in the membrane syste, P is the pressure of the membrane system, V_i is the partial molar volume of Component i in the membrane system, T is the absolute temperature, and P_0 is the reference pressure which is taken as the saturation vapor pressure of the solution mixture. The activity in the liquid permeation process can be taken as a constant. Therefore,

$$n_i^1 = -\frac{1 - \omega_j}{1 - \omega_i - \omega_j} \rho_i m_i v_i \left(\frac{dp}{dx}\right) - \frac{\omega_i}{1 - \omega_i - \omega_j} \rho_j m_j v_j \left(\frac{dp}{dx}\right) \tag{15}$$

Since the coefficients in Eq. (15) are almost pressure-independent in the liquid permeation zone, therefore

$$n_i^{\mathrm{l}} = \left(\frac{1 - \omega_j}{1 - \omega_i - \omega_j}\,\rho_i m_i v_i + \frac{\omega_j}{1 - \omega_i - \omega_j}\,\rho_j m_j v_j\right)\frac{(p_1 - p_0)}{x_1} \tag{16}$$

P_0 is the saturation vapor pressure of the binary mixture solution.

Equation (16) shows that the mass fluxes of components in the zone that behaves as a liquid permeation process is a linear function of feed pressure for a given system.

In the zone that behaves as a vapor permeation process, the chemical potential of individual component is given by Eq. (17):

$$\mu_i = \mu_{i0} + RT \ln a_i \tag{17}$$

Substituting this equation into Eq. (8), we obtain

$$n_i^{\mathrm{v}} = -\frac{1 - \omega_j}{1 - \omega_i - \omega_j}\,\frac{\rho_i m_i RT}{a_i}\left(\frac{da_i}{dx}\right) - \frac{\omega_i}{1 - \omega_i - \omega_j}\,\frac{\rho_j m_i RT}{a_j}\left(\frac{da_j}{dx}\right) \tag{18}$$

Integrating Eq. (18) with boundary conditions, then

$$n_i^{\mathrm{v}} x_{\mathrm{v}} = -RT\int_{(a_{i0},a_{j0})}^{(a_{i2},a_{j2})}\left(\frac{1 - \omega_j}{1 - \omega_i - \omega_j}\,\frac{\rho_j m_i}{a_i}\right)da_i + \left(\frac{\omega_i}{1 - \omega_i - \omega_j}\,\frac{\rho_j m_j}{a_j}\right)da_j \tag{19}$$

where a_{i0} and a_{j0} have the same activity values as those in the liquid feed solution. Equation (19) is a path-dependent line integral, a direct evaluation of this integral is possible only if the relationship between a_i and a_j is known.

The mass flux of Component i with respect to the overall thickness then can be readily derived:

$$\begin{aligned} n_i^{\mathrm{t}} x_{\mathrm{t}} = {} & \left[\left(\frac{1-\omega_i}{1-\omega_i-\omega_j}\rho_i m_i v_i + \frac{\omega_i}{1-\omega_i-\omega_j}\rho_j m_j v_j\right)(p_1 - p_0)\right]_{\mathrm{l}} \\ & + \left[-RT\int_{(a_{i0},a_{j0})}^{(a_{i2},a_{j2})}\left(\frac{1-\omega_j}{1-\omega_i-\omega_j}\,\frac{\rho_i m_i}{a_i}\right)da_i + \left(\frac{\omega_i}{1-\omega_i-\omega_j}\,\frac{\rho_j m_j}{a_j}\right)da_j\right]_{\mathrm{v}} \end{aligned} \tag{20}$$

In a similar way, the mass flux of Component j also can be obtained:

$$\begin{aligned} n_j^{\mathrm{t}} x_{\mathrm{t}} = {} & \left[\left(\frac{1-\omega_i}{1-\omega_i-\omega_j}\rho_j m_j v_j + \frac{\omega_j}{1-\omega_i-\omega_j}\rho_i m_i v_i\right)(p_1 - p_0)\right]_{\mathrm{l}} \\ & + \left[-RT\int_{(a_{i0},a_{j0})}^{(a_{i2},a_{j2})}\left(\frac{1-\omega_i}{1-\omega_i-\omega_j}\,\frac{\rho_j m_j}{a_j}\right)da_j \right. \\ & \left. + \left(\frac{\omega_j}{1-\omega_i-\omega_j}\,\frac{\rho_i m_i}{a_i}\right)da_i\right]_{\mathrm{v}} \end{aligned} \tag{21}$$

The first terms on the right-hand side in both equations are the contribution of the liquid permeation mechanism, and the second term is the contribution of the vapor permeation mechanism. The total mass flux can thus be calculated from the sum of Eqs. (20) and (21).

Under the ideal operation condition, i.e., the permeate pressure is equal to 0 ($a_{i2} = 0$ and $a_{j2} = 0$), evaluation of the permeation flux of Components i and j can be achieved as long as activity dependence of solubility, mobility, and the relationship between a_i and a_j are known. Practically, when the permeate pressure is not equal to 0, then Eq. (20) and (21) combine with the following equations

$$p_2 = p_{i2} + p_{j2} \tag{22}$$

$$\frac{n_i^t}{n_j^t} = \frac{p_{i2}M_i}{p_{j2}M_j} \tag{23}$$

$$a_{i2} = \frac{p_{j2}}{p_i^*} \tag{24}$$

$$a_{j2} = \frac{p_{j2}}{p_j^*} \tag{25}$$

to give a set of equations to solve for the fluxes of the individual components as well as the other desired values. p_i^* and p_j^* are the saturation vapor pressures of pure Components i and j, respectively.

The Relationship between a_i and a_j

Although a tedious and time-consuming iteration method can be used to solve a two-variable differential equation (5, 13, 14), a further simplified calculation procedure is preferred. In order to directly evaluate the integrals of Eqs. (20) and (21), the relationship between a_i and a_j has to be found first. From the Appendix, the relationship between μ_i and μ_j is given by

$$\frac{d\mu_j}{d\mu_i} = C_1 \frac{a_i}{a_j} \tag{26}$$

where C_1 is a constant. Equation (26) can be expressed and rearranged in term of activity as

$$da_j = C_1 da_i \tag{27}$$

which can be further integrated into

$$a_j = C_1 a_i + C_2 \tag{28}$$

The constants C_1 and C_2 can be evaluated from the boundary conditions at position 0: $a_i = a_{i0}$; $a_j = a_{j0}$, and at position 2: $a_i = a_{i2}$; $a_j = a_{j2}$. Therefore,

$$C_1 = \frac{a_{j0} - a_{j2}}{a_{i0} - a_{i2}} \tag{29}$$

and

$$C_2 = \frac{a_{i0}a_{j2} - a_{i2}a_{j0}}{a_{i0} - a_{i2}} \tag{30}$$

This relationship can be applied to Eqs. (20) and (21) to achieve the integral evaluation.

RESULTS AND DISCUSSION

Pervaporation of Hexane–Heptane Mixtures through Polyethylene Membrane

Experimental data for the pervaporation of hexane–heptane mixtures through a polyethylene membrane are available from the literature (2). Simple concentration-dependent solubility and mobility have been assumed and found satisfactory for this membrane system:

$$c_i = K_{ci}a_i \tag{31}$$

$$c_j = K_{cj}a_j \tag{32}$$

$$m_i = K_{mi}(c_i + B_{ji}c_j) \tag{33}$$

$$m_j = K_{mj}(c_j + B_{ij}c_i) \tag{34}$$

where K_{ci} and K_{cj} are the sorption coefficients of Components i and j in the membrane system, respectively, which can be obtained from the solubility of an individual component at unity activity; K_{mi} and K_{mj} are the mobility coefficients of Components i and j in the membrane system, respectively, which can be obtained from the pervaporation test of an individual component; B_{ji} and B_{ij} are the plasticizing factors which account for the effect of one component on the mobility of the other component in the membrane, and they can be obtained from the pervaporation result of binary mixtures.

Figure 2 shows the effect of permeate pressure on the permeation rates for pure hexane (Component i) and pure heptane (Component j) at feed pressure = 1 atm. The theoretical curves are calculated using the PPCSD model for single component permeation (28). The parameter values of sorption and diffusion are

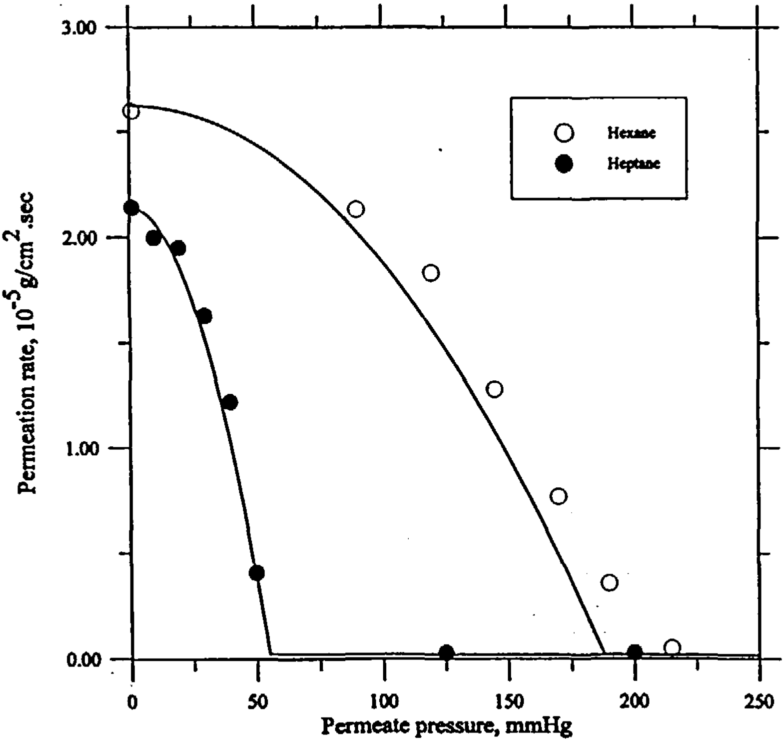

FIG. 2 Permeation rate vs permeate pressure, at feed pressure = 760 mmHg, for pure components. Lines: theoretical calculation; points: experimental data.

$$K_{ci} = 0.128 \text{ g/g polymer}; \; K_{cj} = 0.155 \text{ g/g polymer};$$
$$K_{mi} = 4.75 \times 10^{-13} \text{ gmol·cm}^2\text{/mmHg·cm}^3\text{·s};$$
$$K_{mj} = 2.632 \times 10^{-13} \text{ gmol·cm}^2\text{/mmHg·cm}^3\text{·s}$$

and the other properties required are

$$v_i = 131.6 \text{ cm}^3\text{/gmol}; \; v_j = 147.4 \text{ cm}^3\text{/gmol}; \; P_i^* = 188 \text{ mmHg};$$
$$P_j^* = 55 \text{ mmHg}; \; d_m = 0.9 \text{ g/cm}^3; \; T = 303 \text{ K}; \; x_t = 0.00254 \text{ cm};$$
$$R = 62365.6 \text{ mmHg·cm}^3\text{/gmol·K}$$

where Components *i* and *j* represent hexane and heptane, respectively.

The prediction of the model is in good agreement with the experimentally observed behavior. We use these known values to apply the PPCSD model further for binary mixture permeation.

The pervaporation system we investigate in this paper is hexane–heptane–polyethylene. Since the mixtures of hexane and heptane behave almost ideally, we take the mole fraction of component in mixtures as its activity ($a_i = x_i$; $a_j = x_j$), and the saturation vapor pressure of mixtures can be calculated from Raoult's law: $P^0 = x_iP_i^* + x_jP_j^*$. The only unknown values are the plasticizing factors, B_{ji} and B_{ij}. Greenlaw et al. assumed that both of them are equal to 1 (each component is equally effective in inducing plasticizing) to simplify their theoretical calculation. However, we find that the optimal values should be $B_{ji} = 0.53$ and $B_{ij} = 1.13$ (from best fitting), that is, Component *j* (heptane) exhibits less plasticizing effect on the membrane than does Component *i* (hexane).

Figure 3 shows the effect of permeate pressure on the individual and total permeation rates for a feed concentration of 77 mol% hexane. The saturation

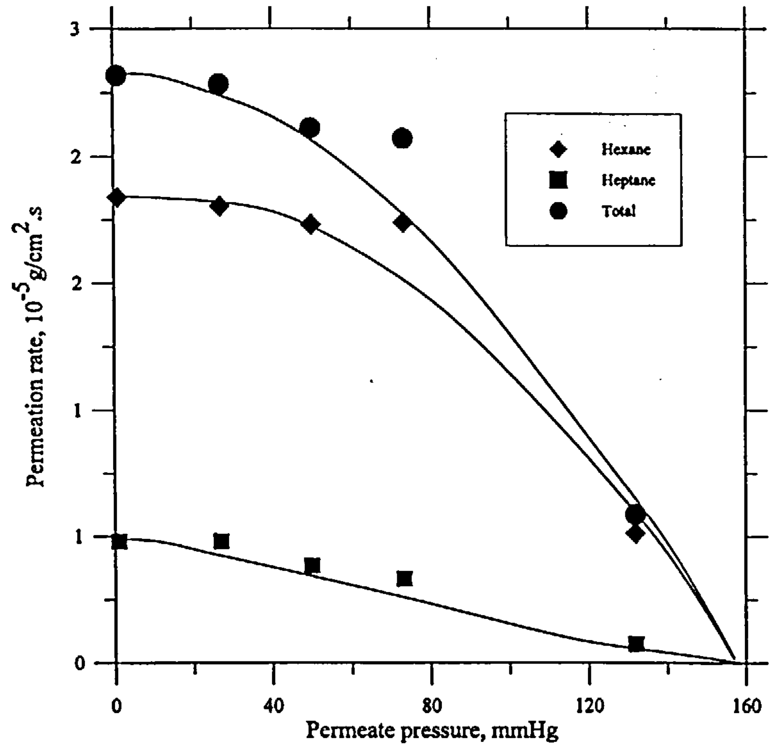

FIG. 3 Permeation rate vs permeate pressure, at feed pressure = 760 mmHg, for hexane–heptane mixture (0.77 mole fraction hexane). Lines: theoretical calculation; points: experimental data.

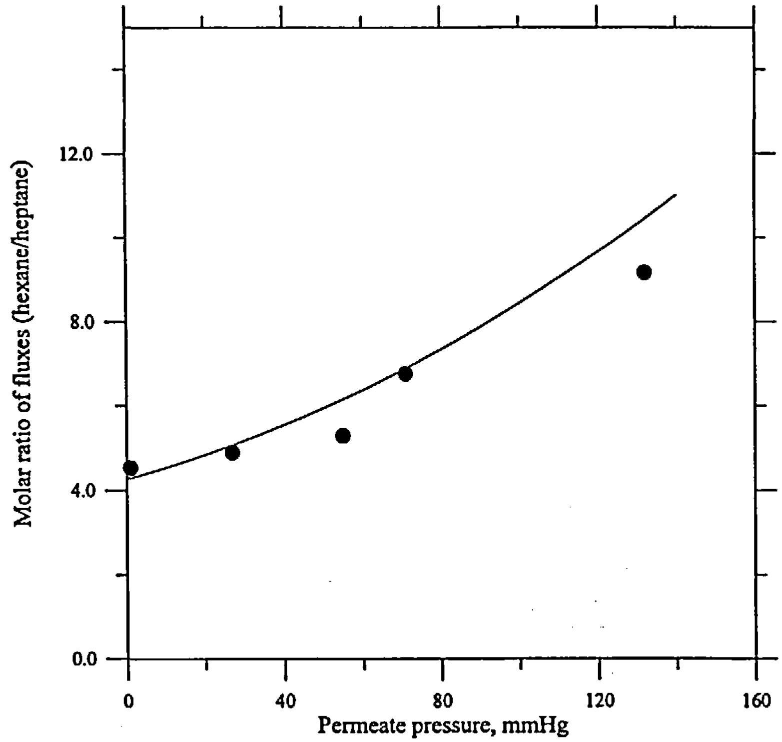

FIG. 4 Molar ratio of fluxes (hexane to heptane) vs permeate pressure, at feed pressure = 760 mmHg, for hexane–heptane mixture (0.77 mole fraction hexane). Line: theoretical calculation; points: experimental data.

vapor pressure of this mixture is 157 mmHg. Both hexane and heptane permeation rates decrease as the permeate pressure increases but with different trends. The permeation rate curve of hexane is convex, whereas the permeation rate curve of heptane is slightly sigmoidal.

Figure 4 shows, but only for the vapor permeate region, the effect of permeate pressure on the molar ratio of hexane to heptane in the permeate for a feed concentration of 77 mol% hexane. In this case the selectivity increases with increasing permeate pressure, while the opposite trend is also found (30), depending on the relative volatility of the permeating components. Comparison between the experimental results and the theoretical curves is in excellent agreement. Note that the theoretical curve derived from the PPCSD model is concave while it is a straight line, well below the experimental data, when predicted from the conventional solution-diffusion model (2).

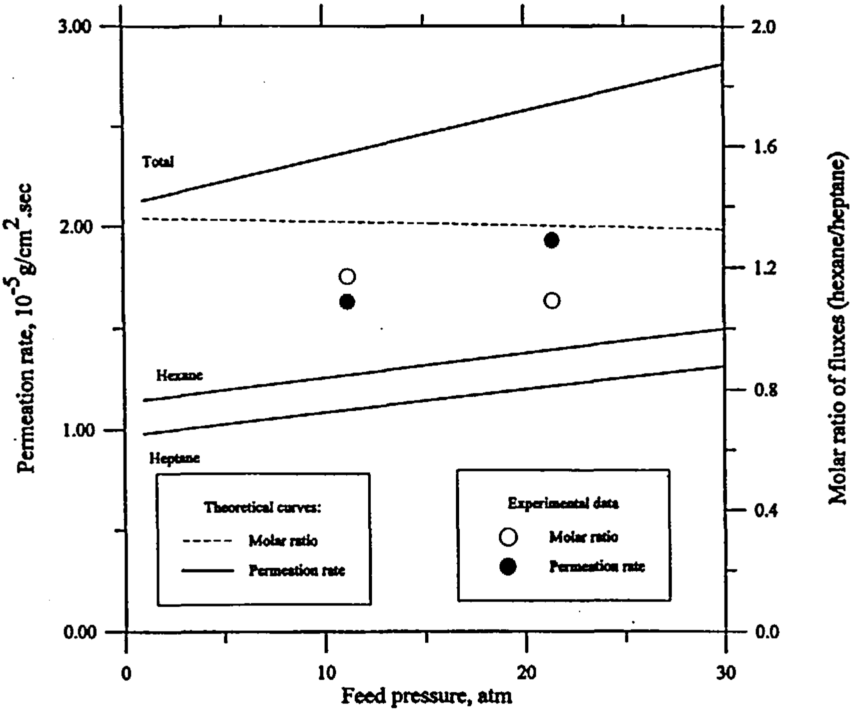

FIG. 5 Permeation rate and molar ratio of fluxes (hexane to heptane) vs feed pressure, at permeate pressure = 1.5 mmHg, for hexane–heptane mixture (0.53 mole fraction hexane). Lines: theoretical calculation; points: experimental data.

Figure 5 shows the effect of feed pressure on the total and individual permeation rates, and the molar ratio of hexane to heptane in the permeate for a feed concentration of 53 mol% hexane (for the theoretical curves). Although the experimental data are not at the same feed concentration, the difference is small (at feed pressure = 11.2 atm, the feed concentration is 56 mol% hexane; at feed pressure = 21 atm, the feed concentration is 53 mol% hexane). This shows that increasing the feed pressure appears to increase the permeation rate and decrease the selectivity. The observed lower permeation rate may result from a more compact membrane structure at a high feed pressure (28).

Figure 6 shows the effect of composition in the feed mixture on the total and individual permeation rates. All the theoretical flux curves are concave, i.e., negative deviation from the ideal situation. Although only one experimental datum is presented, it still agrees pretty well with the calculated curve.

Calculated flux curves without the coupling term are also plotted in this figure. They shows that the coupling flux enhances all the permeation rates. The effect of coupling flux on the permeation rates is determined by the solubility, mobility, and the plasticizing factor as described in the second term of the right-hand side of Eqs. (8) and (9). More detail discussions about the effect of the coupling flux and the plasticizing factor on the pervaporation performance will be presented in the following section.

A plot of separation factor versus mole fraction of hexane in the feed solution is shown in Figure 7. The separation factor is defined as

$$\alpha = \frac{c_i''/c_j''}{c_i'/c_j'} \tag{35}$$

where c' is the mole fraction of component in the feed solution, c'' is the mole

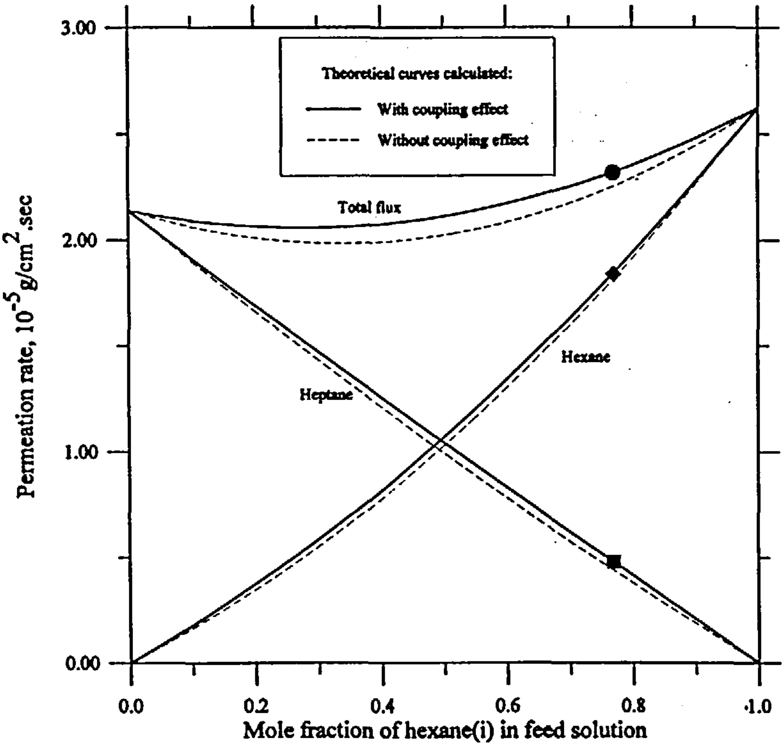

FIG. 6 Permeation rate vs mole fraction of hexane in feed solution, at feed pressure = 760 mmHg, permeate pressure = 1.5 mmHg. Lines: theoretical calculation; points: experimental data.

fraction of component in the permeate vapor, and *i* and *j* are the individual components (in this case, *i* is hexane and *j* is heptane). Calculated curves for both with and without the coupling flux terms are compared with the experimental results, which shows that introduction of the coupling flux terms makes the theoretical prediction closer to the observed results.

The PPCSD model divides the membrane system into a zone that behaves as a liquid permeation proces and a zone that behaves as a vapor permeation process. The contribution of the individual permeation mechanism to the total permeation rate can be theoretically calculated by using Eqs. (20) and (21). We use the above known values to perform the calculation at feed pressure = 760 mmHg. As shown in Fig. 8, at feed concentration = 77 mol% hexane, the contribution of liquid permeation is below 2% until the permeate pressure reaches 100 mmHg, then it increases abruptly to 100% when it reach the

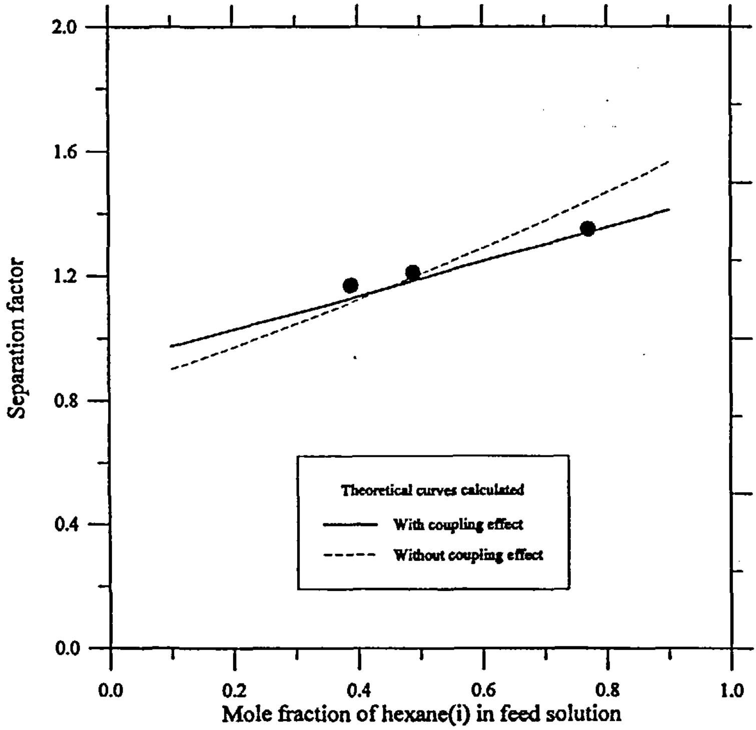

FIG. 7 Separation factor vs mole fraction of hexane in feed solution, at feed pressure = 760 mmHg, permeate pressure = 1.5 mmHg. Lines: theoretical calculation; points: experimental data.

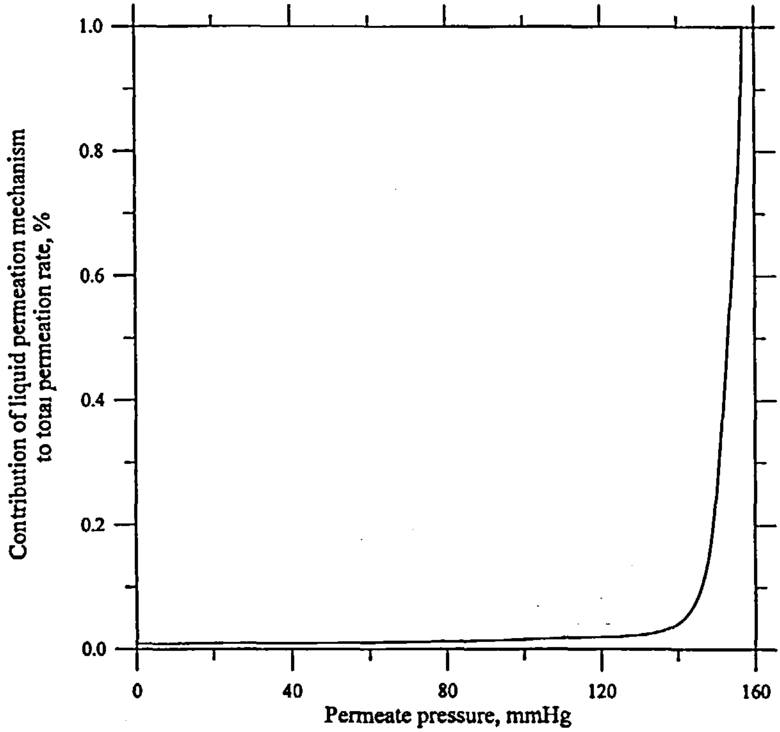

FIG. 8 Contribution of liquid permeation mechanism to total permeation rate vs permeate pressure, at feed pressure = 760 mmHg, for hexane–heptane mixture (0.77 mole fraction hexane).

saturation vapor pressure of the mixture, i.e., 157 mmHg. This result suggests that when pervaporation operates at a reasonably low permeate pressure, part of the liquid permeation in Eqs. (20) and (21) can be neglected compared to that of vapor permeation.

A Study of the Effect of Plasticization and Coupling Flux on Pervaporation

According to the solution-diffusion mechanism, the pervaporation flux is determined by the solubility and diffusivity (or mobility) of permeants in the membrane. If we derive the permeation rate starting from Fick's law, the flux expression of an individual component will end up as a product of concentration-dependent solubility and diffusivity (or mobility), and its own driving force (concentration or chemical potential gradients). The coupling flux was explained to be included in the solubility (thermodynamic part) and the diffusivity (or mobility) (kinetic part) aspects (10, 11). However, from the definition of irreversible thermodynamics (31), the coupling flux results from the driving force of the other components, not by the mutual interaction between the membrane and permeants within its own driving force. Recently, Heintz et al. (13) and Doong et al. (14) used a modified Maxwell–Stefan approach and a generalized Fick's law form, respectively, to model a multicomponent pervaporation system. Both models treat coupling flux in a fashion similar to that defined by irreversible thermodynamics. It can be seen that starting from the mass balance equations, the PPCSD model also derives a set of flux equations equivalent to those obtained in irreversible thermodynamic for binary mixture permeation, which can handle the coupling flux independently.

It can be observed from Eqs. (8) and (9) that the pervaporation flux depends on the solubility and mobility of permeants, as well as the coupling flux. In addition, the coupling flux is also a function of the solubility and mobility of permeants in the membrane. Moreover, the solubility and mobility of permeants in the membrane are influenced by membrane plasticization. In the following discussion we will investigate the effect of plasticization and coupling flux on pervaporation performance through theoretical calculations. To simplify the calculations, the assumption made in the above section is applied and the assumed known values are made according to the fact that a good pervaporation membrane should have a higher solubility and diffusivity for one component in order to achieve separation.

For Component *i* (faster permeant):

$$K_{ci} = 1 \text{ g/g polymer}; \; K_{mi} = 10 \times 10^{-13} \text{ gmol·cm}^2\text{/mmHg·cm}^3\text{·s};$$
$$V_i = 20 \text{ cm}^3\text{/gmol}; \; P_i^* = 50 \text{ mmHg}$$

For Component *j* (slower permeant):

$$K_{cj} = 0.2 \text{ g/g polymer}; \; K_{mj} = 2 \times 10^{-13} \text{ gmol·cm}^2\text{/mmHg·cm}^3\text{·s};$$
$$V_j = 60 \text{ cm}^3\text{/gmol}; \; P_j^* = 100 \text{ mmHg}$$

For the membrane system:

$$P_1 = 760 \text{ mmHg}; \; P_2 = 0 \text{ mmHg}; \; T = 303 \text{ K};$$
$$d_m = 1 \text{ g/cm}^3; \; x_t = 0.01 \text{ cm}$$

Four cases can now be distinguished:

(a) No plasticizing effect for both components ($B_{ji} = 0$, $B_{ij} = 0$).
(b) Weak plasticizing effect for both components ($B_{ji} = 1$, $B_{ij} = 1$).

(c) Weak plasticizing effect for one component and strong plasticizing effect for the other ($B_{ji} = 1$, $B_{ij} = 10$).
(d) Strong plasticizing effect for both components ($B_{ji} = 10$, $B_{ij} = 10$).

The corresponding calculated permeation rates as a function of the activity of Component *i* in a feed solution are shown in Fig. 9. Some conclusions can be drawn from the data in this figure.

1. The stronger the plasticizing effect, the larger is the flux enhancement.
2. Since the plasticizing effect is included in both solubility and mobility, the flux enhancement due to the plasticizing effect is more noticeable for the slower permeant (lower solubility and mobility) than for the faster permeant (higher solubility and mobility).
3. A maximum permeation rate always occurs for the slower permeant due to the effect of the plasticization and coupling flux of the other component.
4. As indicated in Eqs. (8) and (9), the magnitude of coupling flux in the permeation rate of Component *i* is determined mainly by the solubility and mobility of the other component in the membrane. In this calculation the flux enhancement due to the coupling flux is insignificant for the faster permeant, while it is noticeable for the slower permeant, especially in the case of a weaker plasticizing effect.

Figure 10 shows the separation characteristics of the membrane with different plasticizing factors as a function of the activity of Component *i* in the feed solution. At higher activity (or concentration) of Component *i*, the selectivity decreases with increasing plasticizing factors, whereas the selectivity increases when the plasticizing factors increase [comparison of Cases (a), (b), (d)]. The permeation rate of the individual component is influenced by the presence of the other component through plasticizing and coupling. Therefore, when the feed solution is at a higher activity (or concentration) than the other component, the relative flux enhancement of an individual component will become much more significant as the plasticizing factors increase. More often, when the faster permeant exhibits stronger plasticization than does the slower permeant, as in the case of dehydration of organics through hydrophilic membranes, this phenomenon actually changes the membrane performance as shown in Case (c) of Fig. 10.

In summary, the plasticizing effect and the coupling flux do play a very important role in pervaporation performance if the interactions between permeants and the membrane are strong. If we can adjust the interactions in a pervaporation system by employing techniques of polymer blend, crosslinking, etc. to optimize the plasticizing and coupling effects, it is possible to achieve a better membrane performance.

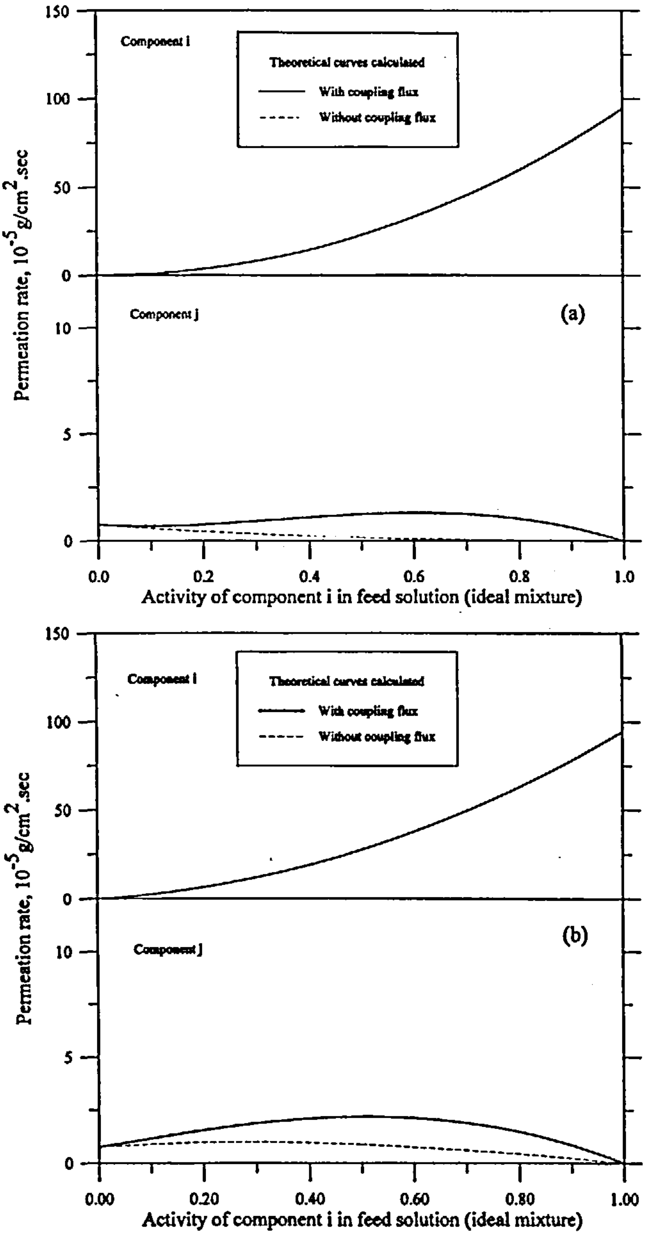

FIG. 9 Permeation rate vs activity of component i in feed solution (ideal mixture), calculated at feed pressure = 760 mmHg, permeate pressure = 0 mmHg. (a) $B_{ji} = 0$, $B_{ij} = 0$; (b) $B_{ji} = 1$, $B_{ij} = 1$; (c) $B_{ji} = 1$, $B_{ij} = 10$, (d) $B_{ji} = 10$, $B_{ij} = 10$.

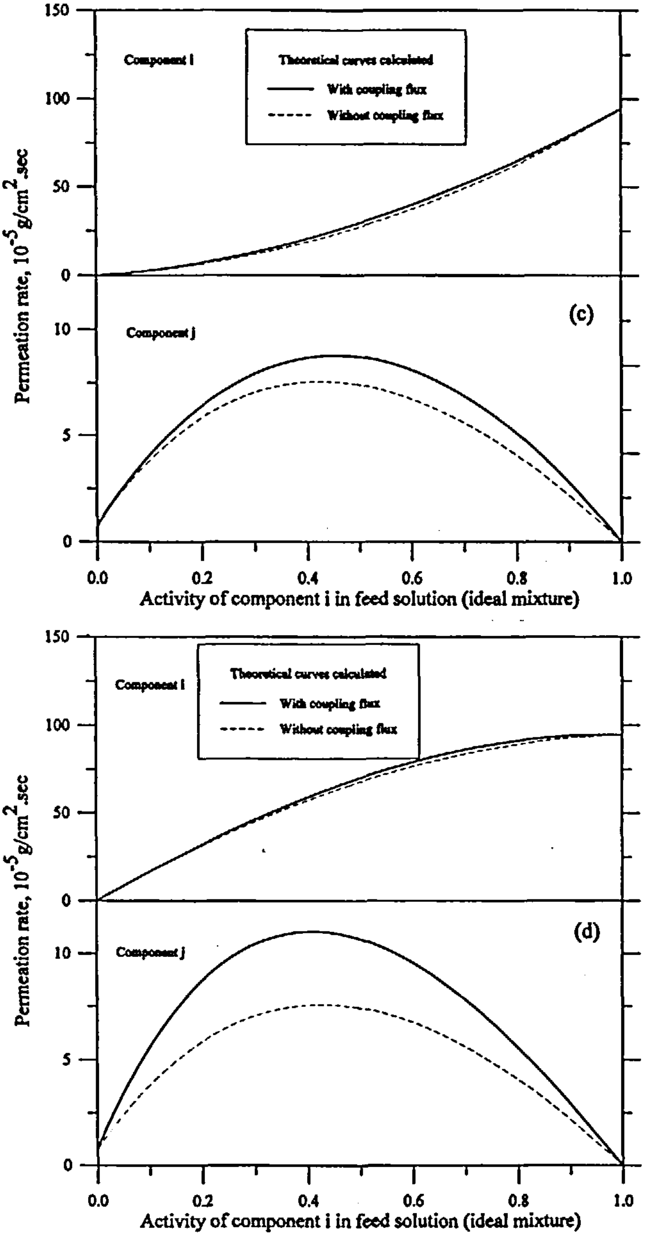

FIG. 9 Continued.

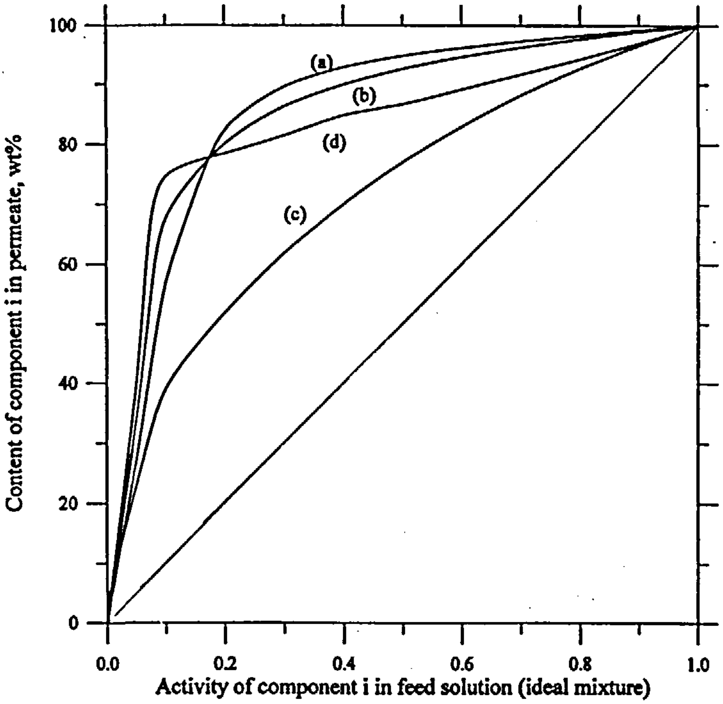

FIG. 10 Content of component *i* in permeate vs activity of component *i* in feed solution, calculated with coupling effect at feed pressure = 760 mmHg, permeate pressure = 0 mmHg. (a) $B_{ji} = 0$, $B_{ij} = 0$; (b) $B_{ji} = 1$, $B_{ij} = 1$; (c) $B_{ji} = 1$, $B_{ij} = 10$; (d) $B_{ji} = 10$, $B_{ij} = 10$.

CONCLUSIONS

The PPCSD model for pervaporation of binary mixtures through a membrane is presented. It is examined by using the experimental data of the hexane–heptane–polyethylene pervaporation system from the literature. Good agreement between observed and calculated membrane performances in terms of the effects of feed pressure, permeate pressure, and feed concentration provide support for the validity of this model. The contribution of the liquid permeation part, a unique feature of the PPCSD model, is rather small compared to that of the vapor permeation part at normal operation conditions (i.e., feed pressure = 760 mmHg and permeate pressure ≈ 0 mmHg). Furthermore, a study of the plasticizing and coupling effects on membrane performance gives insight to the complicated mass transport involved in pervaporation. A slower permeant, usually having lower solubility and mobility, shows a greater increase of flux resulting from a plasticization and coupling effect does than a faster permeant which, in turn, reduces the permselectivity of the membrane.

APPENDIX

Derivation of Relationship between μ_i and μ_j

In the case of binary liquid mixtures, the flux equations from linear nonequilibrium thermodynamics (31) can be rearranged in terms of $d\mu_i/dx$ and $d\mu_j/dx$ to obtain

$$\frac{d\mu_i}{dx} = \frac{n_j L_{ij} - n_i L_{jj}}{L_{jj}L_{ii} - L_{ji}L_{ij}} \tag{A.1}$$

$$\frac{d\mu_j}{dx} = \frac{n_i L_{ji} - n_j L_{ii}}{L_{jj}L_{ii} - L_{ji}L_{ij}} \tag{A.2}$$

A relationship between μ_i and μ_j can be obtained by dividing Eq. (A.2) by Eq. (A.1):

$$\frac{d\mu_j}{d\mu_i} = \frac{n_i L_{ji} - n_j L_{ii}}{n_j L_{ij} - n_i L_{jj}} \tag{A.3}$$

The phenomenological coefficients can be related to Eqs. (8) and (9) in the pseudophase-change solution-diffusion model by

$$L_{ii} = \frac{(1 - \omega_j)\rho_i m_i}{1 - \omega_i - \omega_j}, \qquad L_{jj} = \frac{(1 - \omega_i)\rho_j m_j}{1 - \omega_i - \omega_j}$$
$$L_{ij} = \frac{\omega_i \rho_j m_j}{1 - \omega_i - \omega_j}, \qquad L_{ji} = \frac{\omega_j \rho_i m_i}{1 - \omega_i - \omega_j} \tag{A.4}$$

By substituting Eq. (A.4) into Eq. (A.3) we get

$$\frac{d\mu_j}{d\mu_i} = \frac{\rho_i m_i n_{j\mathrm{D}}}{\rho_j m_j n_{i\mathrm{D}}} \tag{A.5}$$

Applying the Onsager reciprocal relations, i.e., $L_{ij} = L_{ji}$, to Eq. (A.4), we find

$$\frac{\rho_i m_i}{\rho_j m_j} = \frac{\omega_i}{\omega_j} \tag{A.6}$$

Furthermore, assuming $n_{j\mathrm{D}}/n_{i\mathrm{D}}$ is a constant under steady-state pervaporation, Eq. (A.6) can be simplified by substituting the definitions of ω_i and ω_j,

$$\frac{d\mu_j}{d\mu_i} = C\,\frac{c_i}{c_j} \tag{A.7}$$

where C is a constant.

Linear activity-dependent c_i and c_j are assumed in Eqs. (31) and (32). Therefore,

$$\frac{d\mu_j}{d\mu_i} = C_1\,\frac{a_i}{a_j} \tag{A.9}$$

where C_1 is a constant.

SYMBOLS

a	activity of component
d_m	density of the membrane system (g/cm^3)
c	solubility of component in polymer (g/g)
c'	mole fraction of component in feed solution
c''	mole fraction of component in permeate vapor
C_1	constant in Eq. (26)
C_2	constant in Eq. (28)
D	diffusivity of component in membrane system (cm^2/s)
K_c	constant in Eq. (31) (g/g)
K_m	constant in Eq. (32) (gmol·cm^2/mmHg·cm^3·s)
m	mobility of component in membrane system (gmol·cm^2/mmHg·cm^3·s)
n	mass flux of component (g/cm^2·s)
$n_{i\mathrm{D}}$	mass flux of Component *i* due to diffusion (g/cm^2·s)
P	pressure (mmHg)
P_0	reference pressure (mmHg)
P^*	saturation pressure of component (mmHg)
R	ideal gas constant = 62,365.6 mmHg·cm^3/gmol·K
T	absolute temperature (K)
V	partial molar volume of component (cm^3/gmol)
x	thickness of membrane system (cm)

Greek Letters

α	separation factor
μ	chemical potential of component (J/gmol)
μ_{i0}	chemical potential of Component *i* at reference state (J/gmol)
ρ	mass concentration of component in membrane system (g/cm^3)
ω	mass fraction of component in membrane system (g/g)

Subscripts

i	Component i
j	Component j
p	polymer
0	position of interface between liquid and vapor permeation mechanisms
1	position of interface between feed side and membrane system
2	position of interface between permeate side and membrane system

Superscripts

F	feed side
l	liquid permeation mechanism
M	membrane system side
P	permeate side
t	overall
v	vapor permeation mechanism

ACKNOWLEDGMENTS

The financial support of the Natural Sciences and Engineering Research Council (NSERC) of Canada and the Environmental Science and Technology Alliance Canada (ESTAC) are gratefully acknowledged.

REFERENCES

1. F. W. Greenlaw, R. A. Sheldon, and E. V. Thompson, "Dependence of Diffusive Rates on Upstream and Downstream Pressures I. Single Component Permeant," *J. Membr. Sci.*, *2*, 141 (1985).
2. F. W. Greenlaw, R. A. Sheldon, and E. V. Thompson, "Dependence of Diffusive Rates on Upstream and Downstream Pressures II. Two Component Permeant," *Ibid.*, *2*, 333 (1985).
3. T. Q. Nguyen, "Modelling of the Influence of Downstream Pressure for Highly Selective Pervaporation," *Ibid.*, *34*, 165 (1987).
4. R. Rautenbauch and R. Albrecht, "Separation of Organic Binary Mixtures by Pervaporation," *Ibid.*, *7*, 203 (1980).
5. R. Rautenbach and R. Albrecht, "The Separation Potential of Pervaporation. Part 1. Discussion of Transport Equations and Comparison with Reverse Osmosis," *Ibid.*, *25*, 1 (1985).
6. M. Fels and R.Y.M. Huang, "Theoretical Interpretation of the Effect of Mixture Composition on the Separation of Liquid in Polymers," *J. Macromol. Sci.—Phys.*, *B5*(1), 89 (1971).
7. R. Y. M. Huang and J. W. Rhim, "Theoretical Estimations of Diffusion Coefficients," *J. Appl. Polym. Sci.*, *41*, 535 (1990).
8. J. W. Rhim and R. Y. M. Huang, "On the Prediction of Separation Factor and Permeability in the Separation of Binary Mixtures by Pervaporation," *J. Membr. Sci.*, *46*, 335 (1989).

9. C. K. Yeom and R. Y. M. Huang, "Modelling of Pervaporation Separation of Ethanol–Water Mixtures through Crosslinked Poly(Vinyl Alcohol) Membrane," *Ibid.*, *67*, 39 (1992).
10. M. H. V. Mulder and C. A. Smolders, "On the Mechanism of Separation of Ethanol/Water Mixtures by Pervaporation. I. Calculations of Concentration Profiles," *Ibid.*, *17*, 289 (1984).
11. M. H. V. Mulder and C. A. Smolders, "On the Mechanism of Separation of Ethanol/Water Mixtures by Pervaporation. II. Experimental Concentration Profiles," *Ibid.*, *23*, 41 (1985).
12. A. Heintz and W. Stephan, "A Generalized Solution-Diffusion Model of the Pervaporation Process through Composite Membranes. Part I. Prediction of Mixture Solubility in the Dense Active Layer using the UNIQUAC Model," *Ibid.*, *89*, 143 (1994).
13. A. Heintz and W. Stephan, "A Generalized Solution-Diffusion Model of the Pervaporation Process through Composite Membranes. Part II. Concentration Polarization, Coupled Diffusion and the Influence of the Porous Support," *Ibid.*, *89*, 153 (1994).
14. S. J. Doong, W. S. Ho, and R. P. Mastondrea, "Prediction of Flux and Selectivity in Pervaporation through a Membrane," *Ibid.*, *107*, 129 (1995).
15. R. B. Long, "Liquid Permeation through Plastic Films," *Ind. Eng. Chem. Fundam.*, *4*, 445 (1965).
16. R. Y. M. Huang and V. J. C. Lin, "Separation of Liquid Mixtures by Using Polymer Membranes. I. Permeation of Binary Organic Mixtures through Polyethylene," *J. Appl. Polym. Sci.*, *12*, 2615 (1968).17. J. P. Brun, C. Larchet, G. Bulvestre, and B. Auclair, "Sorption and Pervaporation of Dilute Aqueous Solution of Organic Compounds through Polymer Membranes," *J. Membr. Sci.*, *25*, 55 (1985).
18. J. P. Brun, C. Larchet, G. Bulvestre, and B. Auclair, "Modelling of the Pervaporation of Binary Mixtures through Moderately Swelling, Non-reacting Membranes," *Ibid.*, *23*, 257 (1985).
19. S. Sourirajan, S. Bao, and T. Matsuura, "An Approach to Membrane Separation by Pervaporation," in *Proceedings of the 2nd International Conference on Pervaporation Process in the Chemical Industry* (R. Bakish, Ed.), Bakish Materials Corp., Englewood, NJ, 1987.
20. T. Okada and T. Matsuura, "A New Transport Model for Pervaporation," *J. Membr. Sci.*, *59*, 133 (1991).
21. T. Okada, M. Yoshikawa, and T. Matsuura, "A study on Pervaporation of Ethanol/Water Mixtures on the Basis of Pore Flow Model," *Ibid.*, *59*, 151 (1991).
22. T. Okada and T. Matsuura, "Predictability of Transport Equations for Pervaporation on the Basis of Pore-Flow Mechanism," *Ibid.*, *70*, 163 (1992).
23. R. K. Tyagi and T. Matsuura, "Possibility of Concentration Polarization Inside the Membrane during Steady-State Pervaporation, in "*Procredings of the 5th International Conference on Pervaporation Procees in the Chemical Industry* (R. Bakish, Ed.), Bakish Materials Corp., Englewood, NJ, 1991, p. 460.
24. R. K. Tyagi and T. Matsuura, "Concentration Polarization Occurring Inside the Membrane during Steady State Pervaporation," *Chem. Eng, Commun.*, *134*, 157 (1995).
25. R. K. Tyagi, A. E. Founda, and T. Matsuura, "A Pervaporation Model: Membrane Design," *Chem. Eng. Sci.*, *19*, 3105 (1995).
26. O. Kedem, "The Role of Coupling in Pervaporation," *J. Membr. Sci.*, *47*, 277 (1989).
27. M. H. V. Mulder, "Thermodynamic Principles of Pervaporation," in *Pervaporation Membrane Separation Processes* (R. Y. M. Huang, Ed.), Elsevier, Amsterdam, 1991, pp. 225–251.
28. J.-J. Shieh and R. Y. M. Huang, "A Pseudophase-Change Solution-Diffusion Model for Pervaporation I. Single Component Permeation," *Sep. Sci. Technol.*, *33*, 767 (1998).

29. R. B. Bird, W. E. Stewart, and E. N. Lightfoot, *Transport Phenomena*, Wiley, New York, NY, 1960.
30. J. Neel, Q. T. Nguyen, R. Clement, and D. J. Lin, "Influence of Downstream Pressure on the Pervaporation of Water–Tetrahydrofuran Mixtures through a Regenerated Cellulose Membrane (Cuprophan), *J. Membr. Sci.*, *27*, 217 (1986).
31. B. Baranowski, "Non-equilibrium Thermodynamics as Applied to Membrane Transport," *Ibid.*, *57*, 119 (1991).

Received by editor October 11, 1996
Revision received July 1997